ResearchGate

See discussions, stats, and author profiles for this publication at: https://www.researchgate.net/publication/21262814

Olfactomedin: Purification, characterization, and localization of a novel olfactory glycoprotein

ARTICLE *in* BIOCHEMISTRY · OCTOBER 1991

Impact Factor: 3.02 · DOI: 10.1021/bi00102a004 · Source: PubMed

CITATIONS
102

READS
18

5 AUTHORS, INCLUDING:

Bert Ph M Menco
Northwestern University
66 PUBLICATIONS **2,898** CITATIONS

SEE PROFILE

Available from: Bert Ph M Menco
Retrieved on: 29 January 2016

Olfactomedin: Purification, Characterization, and Localization of a Novel Olfactory Glycoprotein†

David A. Snyder,‡ Ann M. Rivers,‡ Hiroko Yokoe,‡ Bert Ph. M. Menco,§ and Robert R. H. Anholt*,‡

Department of Neurobiology, Box 3209, Duke University Medical Center, Durham, North Carolina 27710, and Department of Neurobiology and Physiology, Northwestern University, 2153 Sheridan Road, Evanston, Illinois 60208-3520

Received April 24, 1991; Revised Manuscript Received June 20, 1991

ABSTRACT: We have identified a novel glycoprotein expressed exclusively in frog olfactory neuroepithelium, which we have named "olfactomedin". Olfactomedin is a 57-kDa glycoprotein recognized by seven monoclonal antibodies, previously shown to react solely with proteins of olfactory cilia preparations. It undergoes posttranslational modifications, including dimerization via intermolecular disulfides and attachment of complex carbohydrate moieties that contain *N*-acetylglucosamine and β-D-galactoside sugars. Olfactomedin strongly binds to *Ricinus communis* agglutinin I and has been purified to homogeneity by lectin affinity chromatography. Polyclonal rabbit antiserum raised against purified olfactomedin confirmed that it is expressed only in olfactory tissue. Immunohistochemical studies at the light microscopic and electron microscopic level show that olfactomedin is localized in secretory granules of sustentacular cells, in acinar cells of olfactory glands, and at the mucociliary surface. The massive production of olfactomedin and its striking deposition at the chemosensory surface of the olfactory neuroepithelium suggest a role for this protein in chemoreception.

Chemosensory information from the environment is gathered by olfactory receptor cells, which mediate recognition and discrimination of odorants (Lancet, 1986; Anholt, 1989). These cells are located in the olfactory neuroepithelium. They are bipolar neurons, which project an axon to the olfactory bulb and a dendrite to the nasal lumen. The dendrite forms at its apical end a dilatation, the olfactory knob, which gives rise to a group of chemosensory cilia surrounded by the mucus that lines the nasal cavity. Different odorants activate distinct subpopulations of olfactory receptor cells, thus generating distinct patterns of neuronal activity that encode odor quality and concentration (Duchamp et al., 1974; Sicard & Holley, 1984).

Current evidence supports the notion that odorant recognition and olfactory transduction are initiated at the mucociliary surface. Olfactory cilia are enriched in a tissue-specific form of adenylate cyclase (Pfeuffer et al., 1989; Bakalyar & Reed, 1990), which is regulated by a distinct GTP-binding protein that is closely related to G_s (Pace & Lancet, 1986; Anholt et al., 1987) and has been designated G_{olf} (Jones & Reed, 1989). The activity of this enzyme is enhanced by odorants in a GTP-dependent manner (Pace et al., 1985; Sklar et al., 1986; Shirley et al., 1986; Breer et al., 1990; Boekhoff et al., 1990), and the resulting increase in cyclic AMP opens ion channels (Nakamura & Gold, 1987; Kolesnikov et al., 1990) that are homologous to cyclic GMP activated channels of photoreceptor cells (Dhallan et al., 1990). It is thought that opening of cyclic nucleotide gated channels underlies the generator current, which leads to excitation of olfactory receptor cells (Nakamura & Gold, 1987; Firestein & Werblin, 1989; Firestein et al., 1991; Kurahashi, 1990; Frings & Lindemann, 1991). The observations that calcium activates the olfactory adenylate cyclase via calmodulin (Anholt & Rivers, 1990) and that depletion of intracellular calcium prevents desensitization of olfactory neurons (Kurahashi & Shibuya, 1990) indicate that calcium plays a central role in controlling olfactory transduction (Restrepo et al., 1990). In addition, activation by some odorants results in the formation of inositol triphosphate (Huque & Bruch, 1986; Boekhoff et al., 1990; Restrepo et al., 1990).

Recently, a novel family of G-protein-linked receptors that are expressed uniquely in olfactory tissue and are members of a multigene family was discovered (Buck & Axel, 1991). This multigene family of putative odorant receptors contains most likely several hundred members, and analysis of homologies among members of this family has identified subfamilies within this group of proteins. It has been suggested that such subfamilies may interact with odorants that belong to major structural classes and that individual members of each subgroup may recognize more subtle differences between otherwise structurally similar odorants (Buck & Axel, 1991). Although binding of odorants to this new family of proteins and linkage of these proteins to adenylate cyclase remain to be demonstrated, the tissue specificity of this multigene family of G-protein-linked receptors suggest that they may represent odorant receptors.

Previously, we described a library of monoclonal antibodies (mAbs) raised against olfactory cilia to identify proteins located uniquely at the chemosensory membrane, which, because of their tissue-specific localization, are expected to play important roles in facilitating or mediating odorant recognition (Anholt et al., 1990). We expanded this library to a total of 84 mAbs and identified seven mAbs that recognize proteins that occur only in preparations of olfactory cilia. During the course of our studies it became clear that these mAbs recognize different forms of the same protein, which we have named "olfactomedin". Here, we describe the identification, purification, and initial characterization of this novel olfactory tissue specific protein. Moreover, we demonstrate that olfactomedin is produced by sustentacular cells and submucosal glands and deposited at the chemosensory surface of the olfactory neuroepithelium.

† This work was supported by NIH Grant DC00394 and U.S. Army Research Office Grant DAAL03-89-K-0178 (to R.R.H.A.) and by NSF Grant BNS-8809839 (to B.Ph.M.M.).

* To whom correspondence should be addressed.

‡ Duke University Medical Center.

§ Northwestern University.

0006-2960/91/0430-9143$02.50/0 © 1991 American Chemical Society

Materials and Methods

Preparation of Olfactory Cilia and Membranes from Frog Tissues. Bullfrogs, *Rana catesbeiana*, were obtained from Acadian Biological (Rayne, LA), Lemberger (Oshkosh, WI), and Amphibians of North America (Nashville, TN). Frogs were killed by decapitation, and the dorsal and ventral olfactory epithelia were dissected. Olfactory cilia were detached from the epithelia by calcium shock and subjected to sucrose gradient centrifugation as described previously (Anholt et al., 1986).

Respiratory cilia from the palate were prepared in the same manner, except that the tissue during the calcium shock was subjected to vigorous mechanical agitation for 1 min on a vortexer.

Several millimeter long stretches of olfactory nerve could readily be dissected during removal of the olfactory epithelia. To prepare membranes of olfactory nerve, brain, heart, liver, lung, and kidney, tissues were dissected and homogenized in ice-cold Ringer's solution[1] with a Tekmar Tissumizer for 2 × 30 s. The homogenates were filtered through a double layer of surgical gauze and centrifuged for 20 min at 6500*g* at 4 °C. The pellets were resuspended in Ringer's solution and homogenized and centrifuged as before. Retinal rod outer segments were obtained after dissection of the retinas by gently agitating the tissue for 10 min on an end-over-end shaker at 4 °C in 2 mM HEPES, pH 7.4, 112 mM NaCl, 3.4 mM KCl, and 2.4 mM $NaHCO_3$ (Ringer's solution). The detached retinal rod outer segments were then collected and processed in the same way as olfactory or respiratory cilia.

All membranes were suspended in Ringer's solution and protein concentrations were determined by the method of Lowry et al. (1951) with BSA as standard. The membrane suspensions were aliquoted and stored at −80 °C.

Polyacrylamide Gel Electrophoresis and Immunoblotting. Polyacrylamide gel electrophoresis in SDS was performed on 10% slab gels in the discontinuous buffer system of Laemmli (1970) after treatment of the samples with 2-mercaptoethanol, unless indicated otherwise. Biotinylated standards, including soybean trypsin inhibitor (21.5 kDa), carbonic anhydrase (31 kDa), ovalbumin (45 kDa), BSA (66.2 kDa), phosphorylase B (97.4 kDa), β-galactosidase (116.25 kDa), and myosin (200 kDa), were obtained from Bio-Rad (Richmond, CA), as were prestained standards, including ovalbumin (46.5 kDa), BSA (77 kDa), β-galactosidase (116.5 kDa), and myosin (205 kDa).

Electrophoretic transfer onto nitrocellulose membranes (Schleicher and Schuell, Keene, NH) and immunoblotting were performed exactly as described previously (Anholt et al., 1987). The membranes were blocked by incubation for at least 30 min in 50 mM Tris·HCl, 1 mM EDTA, 0.1% gelatin, and 0.1% Triton X-100 (Boehringer Mannheim, Indianapolis, IN), pH 7.5, and cut into strips. The strips were incubated for at least 1 h with the primary antibody or biotinylated lectin (Vector Laboratories, Burlingame, CA) at the desired concentration in 10 mM sodium phosphate buffer, 150 mM NaCl, and 0.05% (v/v) Tween 20 (Aldrich Chemical Co., Milwaukee, WI), pH 7.5 (PBS/Tween), at 4 °C. Bound antibodies were visualized with biotinylated secondary antibody complexed to avidin and biotinylated HRP (Vector Laboratories) by using 3,3′-diaminobenzidine (Sigma Chemical Co., St. Louis, MO) as the chromogenic substrate. Gels were silver stained by the procedure of Oakley et al. (1980).

Purification of Olfactomedin by Lectin Affinity Chromatography. Since *Ricinus communis* agglutinin I (RCA) binds only to the monomeric form of olfactomedin, ciliary membranes (typically 200 μg of protein) or membranes from deciliated olfactory epithelium (typically 1 mg of protein) were reduced with 0.14 M 2-mercaptoethanol in Ringer's solution for 15 min at 4 °C, followed by centrifugation in a microcentrifuge at 16600*g* for 15 min at 4 °C, prior to solubilization. The pellet was resuspended in Ringer's solution supplemented with 2% CHAPS (Boehringer Mannheim) and incubated on an end-over-end shaker for 30 min at 4 °C. The suspension was centrifuged as before, and the supernatant was diluted with Ringer's solution to a final concentration of 0.2% CHAPS and applied to 25 μL of RCA conjugated to agarose (Vector Laboratories), equilibrated in Ringer's solution containing 0.2% CHAPS. The resin was incubated overnight (16–18 h) at 4 °C on an end-over-end shaker. After centrifugation in a microcentrifuge at 16600*g* for 10 s, the unbound fraction was collected. The resin was washed five times by resuspending it in Ringer's solution containing 0.2% CHAPS, followed by centrifugation. To elute olfactomedin, the resin was incubated for 1 h on a shaker at ambient temperature (22 °C) with 75 μL of 0.5 M D-galactose (Sigma Chemical Co.) and 10 mM 2-mercaptoethanol in Ringer's solution containing 0.2% CHAPS. After the eluate was collected by centrifugation as before, the elution procedure was repeated and the two eluates were combined. The combined eluate was dialyzed overnight at 4 °C against 2 × 500 volumes of distilled water, dried under vacuum by evaporation in a Savant SpeedVac concentrator, and stored at −80 °C. Purity of the preparation was evaluated by SDS–PAGE followed by silver staining and/or immunoblotting. RCA breakdown products were often observed in the eluate (e.g., Figure 2). These could be readily removed, when necessary, with virtual complete recovery of olfactomedin by incubating the eluate with anti-RCA IgG (Vector Laboratories) conjugated to Affigel-10 (Bio-Rad; 2 mg of IgG/mL of gel).

To quantitate recovery of purified olfactomedin from the initial extract, 2-μL aliquots of the extract and the eluate prior to dialysis were blotted onto 0.5 × 0.5 cm squares of nitrocellulose membrane and allowed to dry. The blots were blocked as described above and incubated with a 10-fold diluted ammonium sulfate cut of mAb 8 in PBS/Tween for 1 h at 4 °C. The blots were washed extensively with the same buffer and incubated with ^{125}I-labeled sheep anti-mouse IgG (10 000 cpm/mL; Amersham Corp., Arlington Heights IL) for 1 h at 4 °C. After extensive washing, the blots were allowed to dry and were placed in vials containing scintillation cocktail, and radioactivity was quantitated in a liquid scintillation counter. Counts were linear as a function of ciliary protein, which permitted calculation of the recovery of purified olfactomedin by comparing total immunoreactivity in the eluate with that in the initial extract.

Production of Polyclonal Antiserum against Olfactomedin. Ten to twelve week old (4–5 lb) female New Zealand white rabbits were purchased from Myrtle's Rabbitry (Thompson Station, TN) and maintained in a pathogen-free facility. After collection of preimmune sera, the rabbits were injected in the muscles along the back with olfactomedin purified from 400 μg of ciliary protein, resuspended in 10 mM sodium phosphate buffer and 150 mM NaCl, pH 7.5, and emulsified with an equal volume of complete Freund's adjuvant (Sigma Chemical Co.). Two weeks later the rabbits were immunized again as before, except that incomplete Freund's adjuvant was used,

[1] Abbreviations: PBS/Tween, 10 mM sodium phosphate buffer, 150 mM NaCl, and 0.05% (v/v) Tween 20, pH 7.5; RCA, *Ricinus communis* agglutinin I; Ringer's solution, 2 mM HEPES, 112 mM NaCl, 3.4 mM KCl, and 2.4 mM $NaHCO_3$, pH 7.4; WGA, wheat germ agglutinin.

followed by two additional booster injections at 1-week intervals. The rabbits were exsanguinated under anesthesia, and the serum was collected and fractionated with 45% ammonium sulfate to partially purify the immunoglobulin fraction. After removal of the ammonium sulfate by extensive dialysis against 10 mM sodium phosphate buffer, 150 mM NaCl, and 10 mM NaN_3, pH 7.5, antibodies against RCA breakdown products from the agarose-conjugated RCA could be absorbed on RCA–agarose. IgG could be further purified by affinity chromatography on protein A conjugated to agarose (Sigma Chemical Co.) according to the method of Goudswaard et al (1978).

Antibody Competition Studies. Antibody competition studies were performed by ELISA in 96-well Immulon II microtiter plates (Dynatech Laboratories, Inc., Chantilly, VA). The wells were coated with 50 μL of a suspension of ciliary membranes in 0.1 M sodium bicarbonate buffer, pH 9.6, at a protein concentration of 20 μg/mL. The plates were incubated for 16 h at 37 °C, washed extensively with PBS/Tween, and blocked with 10 mM sodium phosphate buffer, 100 mM NaCl, 10 mM NaN_3, 0.05% (v/v) Tween 20, and 0.2% (w/v) BSA, pH 7.5, for 30 min at 37 °C. The plates were washed five times with PBS/Tween, and triplicate wells were incubated with 50 μL of rabbit antiserum at the desired dilution in PBS/Tween for 2 h at 37 °C. The plates were washed as before, and 50 μL of 10-fold diluted ammonium sulfate cuts of hybridoma supernatants containing the indicated mAbs were placed in the wells. After the mAbs were allowed to bind for 1 h at 37 °C, the plates were washed as before and bound mAb was visualized by using biotinylated horse anti-mouse IgG complexed with avidin and biotinylated HRP (Vector Laboratories) using 2,2′-azinobis(3-ethylbenzothiazoline-6-sulfonic acid) (Sigma Chemical Co.) as the chromogenic substrate. Color formation reflecting bound mAb was measured at 405 nm in an ELISA microtiter plate reader. Maximal binding of mAb was evaluated by substituting preimmune serum for the polyclonal antiserum in the competition assay. Binding of the rabbit antiserum was verified by deleting subsequent incubation with mAb, visualizing bound antibody with biotinylated goat anti-rabbit antiserum (Vector Laboratories, Inc.) and comparing color formation with that observed in wells that received preimmune serum. A 10-fold dilution of ammonium sulfate fractionated supernatant of the parent P3x653.Ag8 myeloma cell line and mAbs that recognize unrelated proteins (mAbs 10, 34, and 78; Anholt et al., 1990) were used to verify that observed competition was specific for mAbs that recognize olfactomedin.

Light Microscopic Immunohistochemistry. Immunohistochemical localization of olfactomedin was performed on 6-μm-thick coronal sections of formalin-fixed decalcified nasal sacs of *R. catesbeiana* embedded in paraffin and mounted on chromalum–gelatin-coated microscope slides. The sections were deparaffinized in xylene and rehydrated through a series of graded alcohols from absolute ethanol to water. The rehydrated sections were incubated with anti-olfactomedin antibodies in PBS/Tween. Incubation with polyclonal antiserum was for 1 h at ambient temperature at a 500-fold dilution of antiserum. Incubations with mAb 43 were overnight (16–18 h) at 4 °C with 10-fold dilutions of ammonium sulfate fractionated hybridoma supernatant. After being washed with PBS/Tween, bound antibodies were visualized with biotinylated secondary antibodies complexed with avidin and biotinylated HRP (Vector Laboratories) using 3,3′-diaminobenzidine tetrahydrochloride and 0.015% (v/v) hydrogen peroxide as substrates. The stained sections were observed under a camera-equipped Leitz Fluovert microscope and photographed with Kodak Ektar 125 color film. To evaluate nonspecific staining, controls were incubated with preimmune serum or ammonium sulfate fractionated medium from the parent P3x653.Ag8 myeloma cell line. Control sections were processed together with the sections of interest in the identical solutions for the same incubation periods.

Electron Microscopy. To visualize olfactomedin immunohistochemically at the electron microscopic level, we used a recently developed freeze-substitution technique, which uses quick-frozen unfixed tissue and allows visualization of the surface of the olfactory epithelium and structures located within 10–15 μm below the epithelial surface (Menco, 1989a,b). Olfactory epithelia were mounted on aluminum disks (Heuser et al., 1979) and within 3 min after dissection were frozen on a liquid nitrogen cooled copper block with the bounce-free Gentleman Jim quick-freeze system (Pelco, Inc., Tustin, CA; Phillips & Boyne, 1984). Freeze-substitution and Lowicryl K11M embedding were carried out as described previously (Menco, 1989a,b; Bridgman & Daley, 1989; Humbel & Schwartz, 1989). Infiltration and low-temperature embedding were done in a CS Auto cryosubstitution apparatus (Leica/Reichert Instruments, Vienna, Austria; Sitte et al., 1986). Anhydrous acetone (EM Sciences, Fort Washington, PA), containing 0.1% uranyl acetate was poured in the substitution chamber, which was kept at −80 °C. Substitution and infiltration lasted 28 days. Embedding lasted 17 days and was carried out in the polar methacrylate-based Lowicryl K11M embedding medium (Chemische Werke Lowi GmbH, Waldkraiburg, Germany; Carlemalm & Villiger, 1989).

All postembedding procedures were carried out at room temperature in multiwell Teflon dishes, which contained water in some of the wells and which were tightly sealed with Parafilm to prevent evaporation (Menco, 1989b). During all incubations, care was taken to expose both sides of the sections by ensuring that grids were completely immersed in the incubation medium. To study the localization of olfactomedin, gold to purple-colored sections were collected on the rough side of 200-mesh, thin bar hexagonal, uncoated nickel grids. For staining with polyclonal antibodies against olfactomedin, grids were preincubated for 2 h in 10 mM Tris·HCl and 500 mM NaCl, pH 8.0, supplemented with 0.1% acetylated BSA (Ac-BSA from Aurion Immunogold Reagents, Wageningen, The Netherlands). For staining with mAb 43, grids were preincubated with the same buffer, supplemented with 10% (v/v) normal goat serum. Following the preincubation, grids were, without intermediate washing, incubated either with protein A–agarose-purified polyclonal anti-olfactomedin antibody (or preimmune serum) at a protein concentration of 0.5 mg/mL in 0.1 M Tris–glycine buffer, pH 7.5, or with ammonium sulfate fractionated hybridoma supernatant containing mAb 43, diluted 5-fold with the same buffer, supplemented with 10% (v/v) normal goat serum, to a protein concentration of 0.1 mg/mL. The samples were incubated overnight at 4 °C in 200-μL snap-cap polystyrene tubes. The grids were jet-washed with 10 mM Tris·HCl and 500 mM NaCl, pH 8.0, and incubated for 2 h with gold-conjugated protein G or gold-conjugated goat anti-mouse IgG/IgM (Biocell Research Laboratories, Cardiff, U.K., or Energy Beam Sciences, Agawam, MA) to visualize binding of rabbit antibodies or mAb 43, respectively. The size of the gold particles was 10 nm, and gold sols were diluted with 20 mM Tris, 150 mM HCl, and 0.1% acetylated BSA to an optical density of about 0.2 at 520 nm, as described previously (Menco, 1989b). Following the incubation with gold-labeled conjugates, the

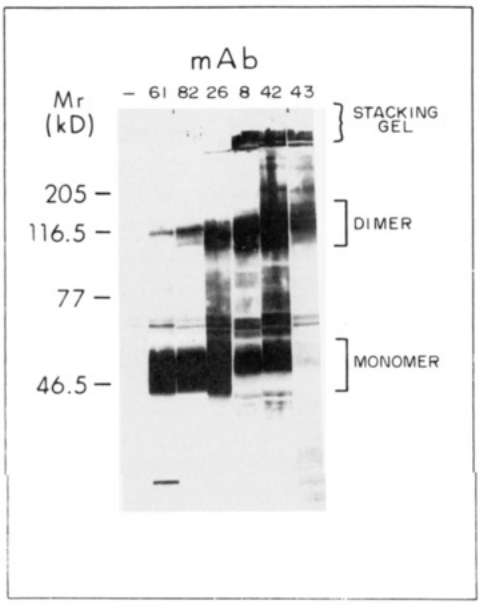

FIGURE 1: Identification of monomeric and dimeric forms of olfactomedin in olfactory cilia preparations by mAbs. Ciliary proteins (100 μg) were reduced with 2-mercaptoethanol and analyzed by Western blotting. Strips of nitrocellulose membrane were incubated overnight with 20-fold dilutions of ammonium sulfate fractionated hybridoma supernatants, containing the indicated mAbs. Since reduction is often not complete, both monomeric and dimeric forms of olfactomedin can be observed. High molecular weight material reflecting aggregates of olfactomedin is evident in the stacking gel on the strips stained with mAbs 8, 42, and 43. Bands that stain nonspecifically are identified on the strip incubated in the absence of mAb. Staining with mAb 45 is not shown, since mAbs 45 and 42 always behave identically.

grids were jet-washed with 10 mM Tris·HCl, 500 mM NaCl, 0.1% (v/v) Tween 20, and 0.01% acetylated BSA, pH 8.0, washed with water, and dried in a desiccator. The sections were stained with filtered 0.5% uranyl acetate in 50% methanol (Bridgman & Daley, 1989) and the section-containing sides of the grids were carbon coated with a Denton evaporator. The specimens were examined at 120 kV with a JEOL 100 CX Temscan electron microscope.

Results

Identification of Multiple Molecular Forms of Olfactomedin. Figure 1 shows immunoreactive patterns of seven mAbs that recognize olfactory tissue specific proteins. MAbs 61 and 82 react predominantly with a broad band centered at 57 kDa. MAbs 26, 8, and 42 reveal immunoreactivity at the same position but in addition show strong staining in the 120-kDa region. In contrast, mAb 43 mainly stains a band in the 120-kDa region. MAbs 8, 42, and 43 also stain high molecular weight material, which is retained in the stacking gel and does not enter the resolving gel (Figure 1). The different immunoreactive species identified by these mAbs reflect different molecular forms of the same protein, which we have named olfactomedin. Evidence which shows that these mAbs all recognize purified olfactomedin and that all of these mAbs compete with monospecific polyclonal antiserum raised against the purified protein is described below (Figures 3 and 4).

Previously, we solubilized ciliary membranes under reducing or nonreducing conditions and analyzed immunoreactive species after sucrose gradient centrifugation to show that the 120-kDa band visualized by mAb 8 represents a disulfide-linked dimer of the 57-kDa species (Anholt et al., 1990). We have extended this analysis to our other antibodies and the results are summarized in Table I. Olfactomedin occurs in its native form as a 120-kDa homodimer, composed of two disulfide-linked 57-kDa monomers. It possesses at least three distinct types of antigenic determinants. Antigenic regions recognized by mAbs 26, 61, and 82 are less accessible in the dimer than in the monomer. In contrast, the determinant for mAb 43 is dependent on integrity of the dimer. Finally, mAbs 8, 42, and 45 recognize both molecular forms (Table I).

Table I: Reactivity of Antibodies with Different Molecular Forms of Olfactomedin

antibody	reactivity with monomer	reactivity with dimer	competition with rabbit antiserum (%)[a]
mAb 8	++	++	34
mAb 26	++	±	57
mAb 42	++	++	29
mAb 43	–	++	98
mAb 45	++	++	nd
mAb 61	++	–	98
mAb 82	++	–	88
rabbit antiserum	++	+	

[a] Percentages of competition between rabbit antiserum and mAbs are calculated from Figure 5 at 10% rabbit antiserum. nd, not determined. Reactivity of mAbs with monomeric and dimeric forms of olfactomedin is determined after solubilization of ciliary membranes by separating monomeric and dimeric forms of olfactomedin by sucrose gradient centrifugation and analyzing immunoreactivity with mAbs in the fractions by Western blotting, as previously described (Anholt et al., 1990).

Purification of Olfactomedin. When we realized that all of our seven mAbs, described above, might recognize the same protein, we decided to purify this interesting, highly immunogenic protein. Initial methods based on immunosorbents were unsuccessful; therefore, we investigated lectin affinity chromatography as an alternative approach. Since olfactomedin contains carbohydrate moieties (Anholt et al., 1990), we examined the reactivity of this protein with con A, wheat germ agglutinin (WGA), and RCA. Of these three lectins, WGA and RCA showed intense staining mainly in the region that corresponds to the position of the 57-kDa monomeric form of olfactomedin. We took advantage of the reactivity of RCA with olfactomedin for its purification.

Preparations of olfactory cilia or deciliated olfactory epithelial membranes were treated with 2-mercaptoethanol to convert most of the olfactomedin to its monomeric form, since RCA preferentially binds to the monomer. After solubilization of the ciliary membranes with 2% CHAPS, the extract was incubated with RCA–agarose. Olfactomedin is virtually the only protein in the extract that binds tightly to RCA–agarose, from which it can be eluted with 0.5 M galactose in the presence of 10 mM 2-mercaptoethanol (Figure 2, lanes 1–3). Neither the sugar nor the reducing agent alone is able to elute the protein from the resin. Addition of 2-mercaptoethanol to the sugar solution facilitates elution, most likely by causing some breakdown of the agarose-conjugated RCA. Silver staining shows a single band at 57 kDa along with two or three bands between 32 and 36 kDa, which can be readily identified as breakdown products of the agarose-conjugated RCA (Figure 2, lane 4). The 57-kDa polypeptide also stains with mAb 61 (Figure 2, lane 5), which conclusively identifies it as olfactomedin.

The yield of olfactomedin in the eluate was estimated from binding of mAbs to olfactomedin on dot blots, which was quantitated with ^{125}I-labeled secondary antibody, and was 57 ± 9% (n = 6) compared to olfactomedin in the initial extract. In our initial experiments olfactory cilia preparations served as the source for olfactomedin. Subsequently, we realized that, using the identical procedure, olfactomedin can also be purified

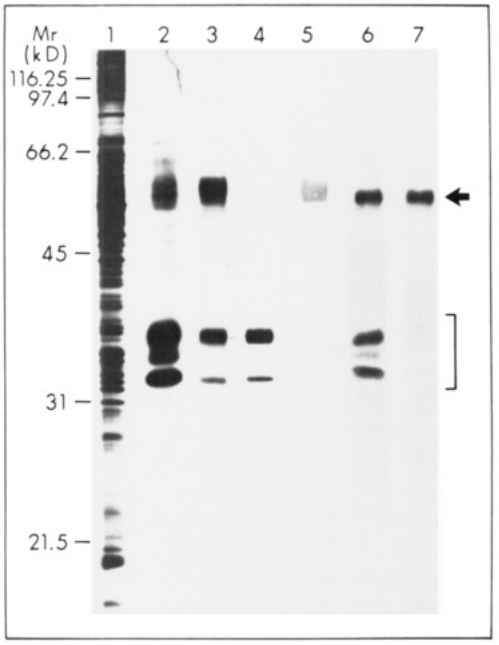

FIGURE 2: Purification of olfactomedin by lectin affinity chromatography. To purify olfactomedin, 200 μg of protein of either olfactory cilia or deciliated epithelial membranes was extracted and the extract subjected to affinity chromatography on RCA–agarose. Lanes 1–3 show silver-stained polyacrylamide gels of the initial extract of olfactory cilia (corresponding to 5 μg of ciliary protein before solubilization; lane 1) and the eluates from RCA–agarose obtained after affinity chromatography of a ciliary extract (lane 2) or an extract from deciliated epithelial membranes (lane 3). Lanes 2 and 3 contain one-tenth of the total volume of the eluates. Lane 4 shows a silver-stained lane that received one-tenth of a similar eluate obtained from RCA–agarose treated identically but not exposed to olfactory proteins. Lane 5 shows a Western blot, with the same amount of eluate, on which olfactomedin is visualized by immunoblotting with a 10-fold dilution of ammonium sulfate fractionated hybridoma supernatant containing mAb 61. Lanes 6 and 7 show staining of the same olfactomedin preparation with 1000-fold diluted anti-olfactomedin rabbit antiserum before and after treatment of the antiserum with RCA–agarose, respectively. The arrow indicates the position of the 57-kDa monomer of olfactomedin, and the bracket indicates the position of RCA breakdown products. Doublet formation of the olfactomedin band is sometimes observed and may be due to reduction of intramolecular disulfide bonds (Anholt et al., 1990).

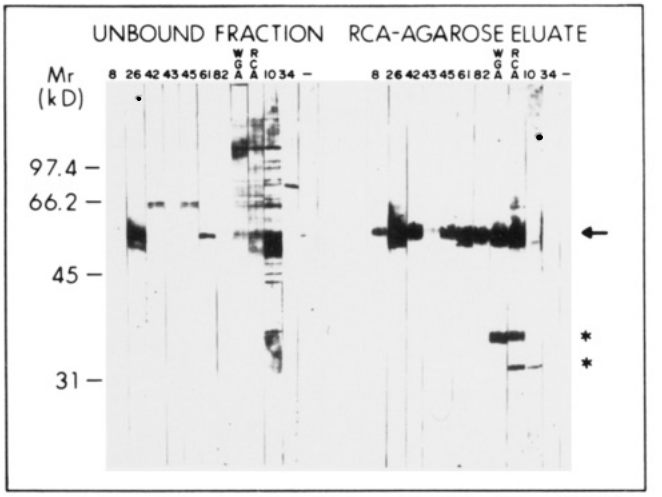

FIGURE 3: Reactivity of purified olfactomedin with mAbs and lectins. To purify olfactomedin, 800 μg of ciliary protein was extracted and subjected to affinity chromatography on RCA–agarose. Forty percent of either the unbound fraction or the RCA–agarose eluate was analyzed by immunoblotting. Strips of the nitrocellulose membrane were stained with 20-fold dilutions of ammonium sulfate fractionated hybridoma supernatants containing the indicated mAbs or with biotinylated WGA (10 μg/mL) and biotinylated RCA (20 μg/mL). MAbs 10 and 34 are antibodies that do not react with olfactomedin (Anholt et al., 1990). A 20-fold dilution of ammonium sulfate fractionated supernatant from the P3x653.Ag8 parent myeloma cell line was used to assess nonspecific immunoreactivity. Note that polypeptides reactive with mAbs 8, 26, 42, 45, 61, and 82 and with WGA and RCA are depleted from the unbound fraction. Immunoreactivity of mAbs 8, 26, 42, 45, 61, and 82 and reactivity with the lectins is recovered in the eluate in the 57-kDa region (indicated by the arrow). In contrast, immunoreactivity against mAbs 10 and 34 is found in the unbound fraction but not in the eluate. The asterisks indicate RCA breakdown products (see also Figure 2).

from deciliated olfactory epithelial membranes, which represent a richer and more economic source. Approximately 200 μg of purified olfactomedin is routinely obtained from approximately 4 mg of epithelial membranes. Taking into account the yield of olfactomedin after affinity chromatography and the presence of some RCA breakdown products that may contaminate the initial RCA eluate, we estimate that olfactomedin may represent up to 5% of the total protein of olfactory epithelial membranes, indicating that it is an abundant component of the olfactory neuroepithelium.

Characterization of Antibody Reactivity with Purified Olfactomedin. To provide further evidence that the monoclonal antibodies, described above, indeed all react with olfactomedin, we characterized their reactivity with the purified protein (Figure 3). Immunoreactivity of mAbs 8, 26, 42, 45, 61, and 82 is depleted from the unbound fraction of the RCA-agarose and is recovered in the eluate. All mAbs react with the purified 57-kDa monomer of olfactomedin (Figure 3). Since olfactomedin is converted into its monomeric form prior to affinity chromatography on RCA–agarose, immunoreactivity of mAb 43, which is dimer-specific, is lost (Figure 3). Evidence that mAb 43 indeed recognizes the same protein is presented below. In contrast, mAbs that bind to unrelated proteins (mAb 10 and 34; Anholt et al., 1990) react with polypeptides in the unbound fraction but do not show immunoreactivity with the eluate of the RCA–agarose (Figure 3). The 57-kDa species in the eluate, as expected, also reacts with biotinylated WGA and RCA (Figure 3), indicating the presence of *N*-acetylglucosamine and β-D-galactoside sugars as part of its carbohydrate moiety.

To provide further evidence that our mAbs all recognize the same protein, we raised antibodies in rabbit against purified olfactomedin and investigated to what extent our mAbs can compete with this antiserum for binding to olfactomedin.

We obtained a monospecific antiserum that reacts preferentially with the monomeric form of olfactomedin, but at 5–10-fold higher concentrations also binds to the dimer (Table I). The antiserum raised against the eluate of the RCA–agarose resin reacts both with the 57-kDa form of olfactomedin and the RCA breakdown products present in the eluate (Figure 2, lane 6). Passage of the antiserum through RCA–agarose eliminates reactivity with the bands between 32 and 36 kDa, again identifying these contaminants as RCA breakdown products, while leaving the immunoreactivity against olfactomedin intact (Figure 2, lane 7). The demonstration that the anti-olfactomedin antiserum reacts monospecifically with a single 57-kDa polypeptide again attests to the purity of olfactomedin after lectin affinity chromatography.

Preincubation of ciliary membranes with rabbit antiserum reduces the binding of all mAbs but to different extents (Figure 4, Table I). Immunoreactivity of mAbs 43, 61, and 82 can be completely blocked by the polyclonal antiserum. In contrast, only about one-third of the immunoreactivity of mAbs 8 and 42 can be inhibited, whereas inhibition of the binding of mAb 26 follows an intermediate pattern (Figure 4, Table I). Reactivity of mAbs that recognize ciliary proteins unrelated

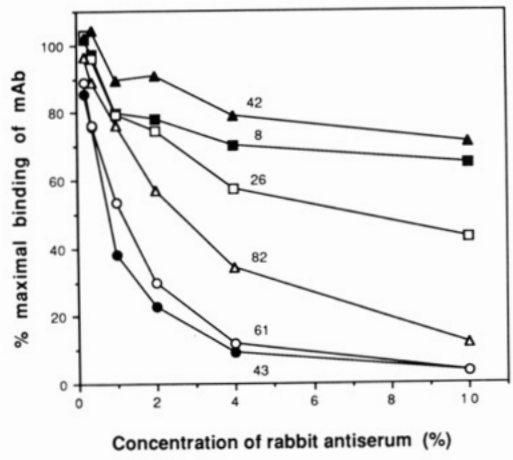

FIGURE 4: Competition between polyclonal antiserum against olfactomedin and mAbs. Microtiter plates were coated with ciliary proteins and incubated sequentially with polyclonal antiserum and mAbs, as described under Materials and Methods. All experiments were done in triplicate. The data are the average of two independent experiments. Measurements of individual points varied less than 5%. Binding of mAbs unrelated to olfactomedin was unaffected by preincubation with anti-olfactomedin rabbit antiserum.

to olfactomedin is unaffected by the antiserum against olfactomedin (Figure 4, legend). Failure of the antiserum to completely inhibit immunoreactivity of mAbs 8 and 42 indicates that antibodies to these antigenic determinants are represented to a lesser extent in the polyclonal antiserum than those that recognize determinants reactive with mAbs 43, 61, and 82. These data provide independent confirmation that all these mAbs, including mAb 43, and the polyclonal antiserum recognize the same molecular entity.

Localization of Olfactomedin. We used our rabbit antiserum against purified olfactomedin to re-assess its tissue specificity prior to immunohistochemistry. The antiserum visualizes the characteristic 57-kDa band of olfactomedin only in preparations of olfactory cilia (or deciliated olfactory epithelial membranes) but not in membranes of olfactory nerve, kidney, heart, liver, respiratory cilia, lung, and brain (Figure 5, left panel). Similarly, no immunoreactivity is found in retinal rod outer segments, which are cilia-derived sensory organelles of photoreceptor cells, although the α and β subunits of transducin are readily identifiable (Figure 5, right panel). These data support the notion that olfactomedin indeed is expressed uniquely in olfactory epithelium.

To visualize olfactomedin in the olfactory neuroepithelium we performed immunohistochemical studies at both the light microscopic and electron microscopic level. We obtained coronal sections through the frog nasal cavity with a largely intact ciliary surface, which under high magnification reveal individual olfactory cilia (Figure 6A). Observation of the epithelial surface after incubation of the sections with biotinylated RCA shows association of the lectin with olfactory cilia together with a lower band of dense staining on top of the epithelial surface (Figure 6B). Within the neuroepithelium, a periodic pattern of granular staining is observed underneath the surface, consistent with the localization of secretory granules of sustentacular cells. Microvilli of sustentacular cells could not be resolved under these conditions.

Staining with polyclonal rabbit antiserum against olfactomedin reveals intense staining of the ciliary surface along with staining in the lower two-thirds of the epithelium and nonuniform staining of the acini of submucosal glands (Figure 6C). Association of olfactomedin with cilia can be observed in regions where the mucociliary surface has become partially detached from the neuroepithelium, allowing clear visualization of individual cilia (Figure 6D). Nonuniform staining of the glands is mostly restricted to the apical regions of acinar cells of submucosal glands (Figure 6E) and is less evident in Bowman's glands that penetrate into the neuroepithelium.

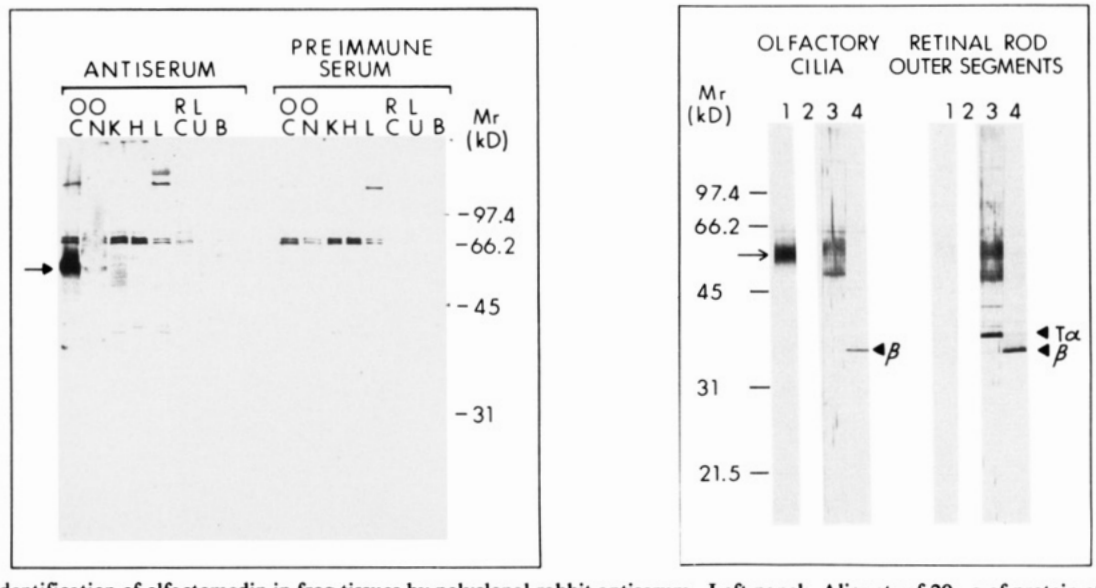

FIGURE 5: Identification of olfactomedin in frog tissues by polyclonal rabbit antiserum. Left panel: Aliquots of 20 μg of protein of preparations of olfactory cilia (OC), respiratory cilia (RC), or membranes of olfactory nerve (ON), kidney (K), heart (H), liver (L), lung (LU), and brain (B) were subjected to PAGE and immunoblotting with a 1000-fold dilution of rabbit antiserum raised against purified olfactomedin or preimmune serum. The arrow indicates the position of the 57-kDa monomeric form of olfactomedin identified only in olfactory cilia preparations. Right panel: Olfactory cilia or retinal rod outer segments, 100 μg each, were subjected to immunoblotting. Strips of the nitrocellulose membrane were stained with a 1000-fold dilution of polyclonal antiserum against olfactomedin (strip 1) or preimmune serum (strip 2). Strips 3 and 4 were stained with a 400-fold dilution of a monospecific antiserum against the α subunit of transducin and a 10000-fold dilution of a monospecific antiserum against the β subunit of GTP-binding proteins, respectively. The antisera against the α subunit of transducin and the β subunit of GTP-binding proteins were of the same batch previously provided by Dr. Susanne M. Mumby (University of Texas, Dallas, TX) designated U-42 and U-49, respectively (Anholt et al., 1987). Note that olfactomedin, indicated by the arrow, is readily demonstrated in preparations of olfactory cilia but not in retinal rod outer segments. In contrast, the 40-kDa α subunit of transducin (Tα) is present in retinal rod outer segments but not in olfactory cilia preparations. The β subunit of GTP-binding proteins, as expected, is identified in both samples at 36 kDa.

Connective tissue, blood vessels, and nerve fascicles are not stained by the antiserum. Incubation of sections with the same concentration of preimmune serum shows some faint staining in the lower two-thirds of the neuroepithelium but no staining at all of the epithelial surface or the glands (data not shown).

Staining of the epithelium with the dimer-specific mAb 43 shows a similar pattern (Figure 6F). Again staining is most evident at the ciliary surface, in the lower two-thirds of the neuroepithelium, and at the luminal regions of acinar cells of submucosal glands (Figure 6, panels F, G, and H). Figure 6G clearly shows heterogeneous punctate association of olfactomedin with olfactory cilia. Incubation of sections with medium from the parent lymphoma cell line, which does not produce mAb, does not result in staining (Figure 6I). As in the case of rabbit antiserum, no staining is observed in nerve fascicles, blood vessels, or connective tissue in the lamina propria. Staining is also not readily detected in Bowman's glands located within the neuroepithelium.

To examine the localization of olfactomedin at the epithelial surface in greater detail, we did immunohistochemical experiments at the electron microscopic level on unfixed freeze-substituted samples using gold-labeled protein G to visualize bound polyclonal antibody or gold-labeled goat anti-mouse IgG/IgM to visualize bound mAb 43 (Figure 7). Both the polyclonal antibodies and mAb 43 show that olfactomedin is localized in the mucus, surrounding the proximal regions of olfactory cilia, the dendritic knobs and microvilli of sustentacular cells, and in secretory granules of sustentacular cells (Figure 7A–C). Two distinct mucous layers can readily be distinguished (Reese, 1965; Menco, 1980). Most of the gold particles, reflecting olfactomedin, are observed in the lower smooth mucous layer. This discrete staining pattern is not observed when sections are incubated with preimmune serum (Figure 7D) or with hybridoma supernatant from the parent cell line, which does not produce mAb against olfactomedin (data not shown).

The combined data obtained from light microscopic and electron microscopic studies indicate that olfactomedin is produced by olfactory glands and sustentacular cells and deposited at the mucociliary surface of the olfactory neuroepithelium.

Discussion

We have identified a novel protein, which appears to be produced by glands and sustentacular cells of frog olfactory epithelium and deposited at the mucociliary surface. This 57-kDa protein undergoes posttranslational modifications, including dimerization via intermolecular disulfides and attachment of complex carbohydrate moieties that contain *N*-acetylglucosamine and galactose-derived sugars. The conspicuous deposition of this protein near the sites where odorant recognition occurs suggests an important role for this protein in olfaction. We have, therefore, named this protein olfactomedin.

To identify olfactomedin we used mAbs previously shown to react solely with proteins of olfactory cilia preparations (Anholt et al., 1990; Table I). Olfactomedin dominates the immunogenicity of olfactory cilia preparations and is recognized by all of these mAbs. The differential reactivity of the mAbs with different molecular forms of olfactomedin initially obscured the fact that they all recognize the same protein. Purification of olfactomedin and the demonstration that all of the mAbs, with the exception of mAb 43, which is dimer-specific, recognize the purified protein provided conclusive evidence that these mAbs indeed all bind to olfactomedin (Figure 3). This is further supported by competition experiments, which show that polyclonal antiserum raised against purified olfactomedin can block, albeit to different extents, binding to ciliary proteins of all of the mAbs, including mAb 43 (Figure 5).

Purification of olfactomedin with RCA–agarose was found to be less problematic than affinity chromatography with immunosorbents and provided a convenient and rapid method to obtain purified olfactomedin with a good yield. The only disadvantage of this technique is the necessity to reduce olfactomedin to its monomeric form, which may affect its as yet unknown function, and the presence of some breakdown products of RCA in the eluate. These breakdown products can, however, be readily removed by absorption to anti-RCA IgG conjugated to agarose (data not shown).

Olfactomedin undergoes posttranslational modifications, including the attachment of unique carbohydrate (Figure 3). Previously, we showed that most of our mAbs, including mAbs 8, 42, and 43, recognize immunogenic determinants that are obliterated after treatment with endoglycosidase H (Anholt et al., 1990). It was, therefore, not surprising for us to find that our antibodies are species-specific and do not cross-react with rat olfactory tissue. This may reflect the dominance of species-specific carbohydrate moieties as immunogenic determinants and does not exclude the occurrence of olfactomedin in other species. Further evidence for the unique composition of olfactomedin's carbohydrate is our finding that olfactomedin reacts with WGA and RCA. In fact, olfactomedin is virtually the only protein that binds to RCA, in stark contrast to the reactivity of con A, which binds to a large array of ciliary proteins (Anholt et al., 1986).

MAbs that recognize olfactomedin can be classified in three categories (Table I): monomer-specific mAbs (26, 61, and 82), dimer-specific mAbs (43), and mAbs that bind to both molecular forms (8, 42, and 45). The reactivity of RCA with olfactomedin resembles that of mAbs 26, 61, and 82 in that it binds preferentially to the monomer. Binding sites for RCA and mAbs 26, 61, and 82 may be inaccessible due to steric hindrance resulting from dimer formation. In contrast, dimerization of olfactomedin appears to be a prerequisite for the formation of the antigenic site for mAb 43. It is of interest to note that polyclonal antiserum raised against the monomeric form of olfactomedin recognizes the monomer preferentially, although it also reacts with the dimer but at higher concentrations.

We used a monospecific polyclonal rabbit antiserum to verify the tissue specificity of olfactomedin. Olfactomedin was readily detectable in olfactory cilia preparations but not in preparations of nonchemosensory cilia from respiratory tissue or of other sensory cilia, such as retinal rod outer segments. Neither did we detect olfactomedin in other mucus-lined tissues, such as lung, glandular tissues, like liver, or membranes from olfactory nerve, brain, kidney, or heart (Figure 4). Although we cannot exclude the occurrence of olfactomedin in other tissues not tested, the complete absence of immunoreactivity in these eight tissues supports the notion that the expression of olfactomedin is specific for olfactory tissue.

We examined the localization of olfactomedin in olfactory neuroepithelium by immunohistochemistry at both the light microscopic and electron microscopic level. From these studies it appears that olfactomedin is not expressed in olfactory receptor neurons but rather is secreted by sustentacular cells and olfactory glands and deposited at the ciliary surface. A punctate pattern of nonuniform deposits of stain along the cilia is evident on sections of olfactory epithelium stained with biotinylated RCA or with antibodies against olfactomedin

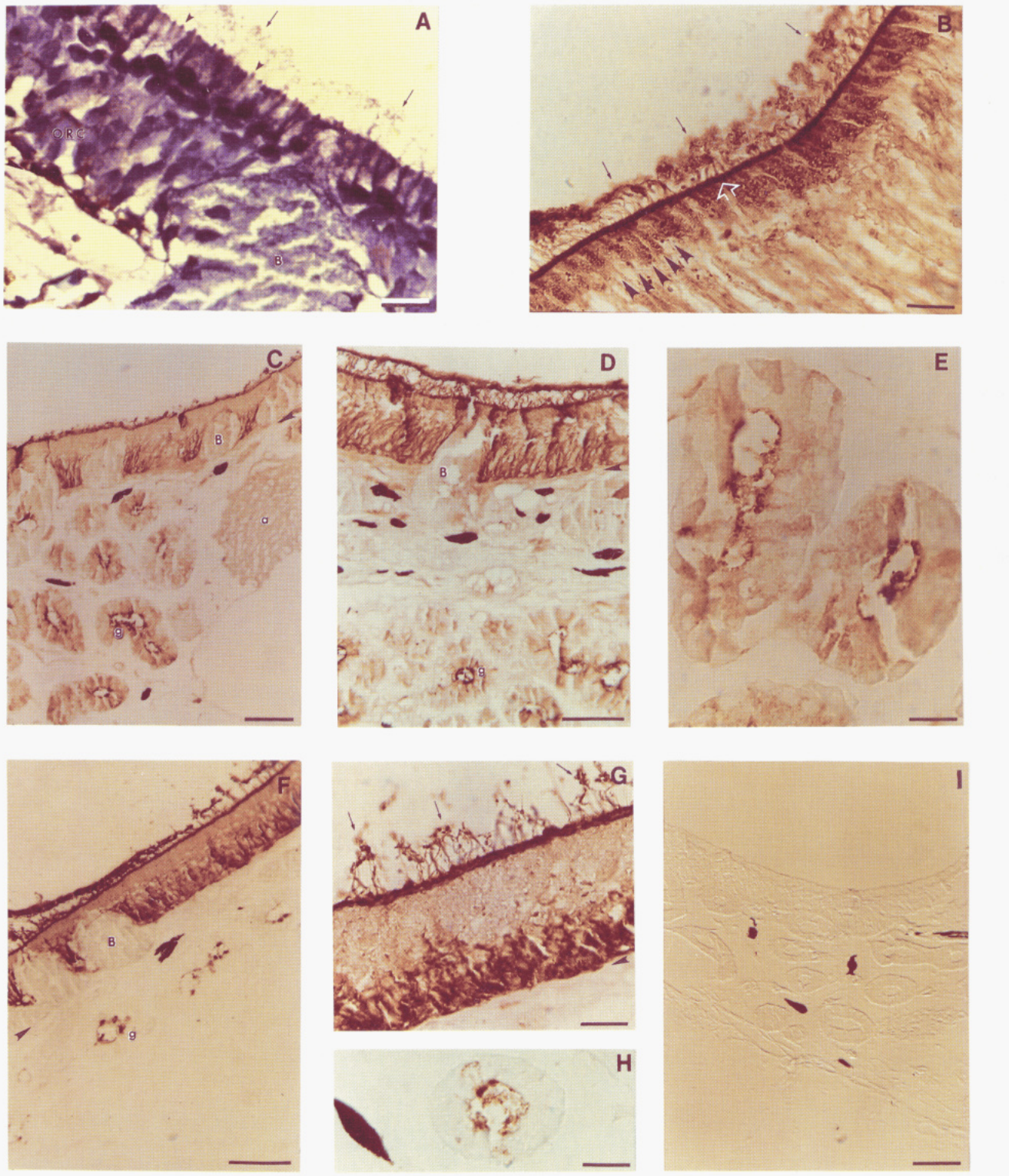

FIGURE 6: Immunohistochemical localization of olfactomedin. Coronal sections through the olfactory sacs of *R. catesbeiana* were stained with toluidine blue (A), 25 μg/mL biotinylated RCA (B; 1-h incubation period), rabbit antiserum against olfactomedin (C, D, and E), mAb 43 (F, G, and H), and hybridoma supernatant from the parent myeloma cell line, which does not produce mAb against olfactomedin (I). Panel I was photographed under Hoffman optics to allow visualization of unstained epithelial structures. Individual cilia are readily observed in panels A, B, and G (small arrows). The location of the basement membrane, which separates the neuroepithelium from the lamina propria, is indicated by large arrowheads. Small arrowheads in panel A indicate olfactory knobs. Note the periodic staining near the epithelial surface (arrowheads) in panel B. The open arrow in panel B shows heavy staining at the epithelial surface. ORC designates olfactory receptor cell bodies; B, Bowman's gland; g, submucosal glands; a, axon bundles. Pigmented heteromorphous structures in the lamina propria represent melanophores. Bars represent 20 μm in panels A, B, E, G, and H and 80 μm in the other panels.

(Figure 6B,G). In addition, olfactomedin is recovered in the olfactory cilia preparation, even after purification of ciliary membranes by sucrose gradient centrifugation. It can be extracted from the ciliary membranes with detergents and tends to form aggregates even in detergent solution, indicating a prominent hydrophobic domain (Figure 1; Anholt et al., 1990). The immunohistochemical patterns of staining and the recovery of olfactomedin in partially purified preparations of olfactory cilia, which persists after sucrose gradient centrifugation, suggest a specific interaction between olfactomedin and

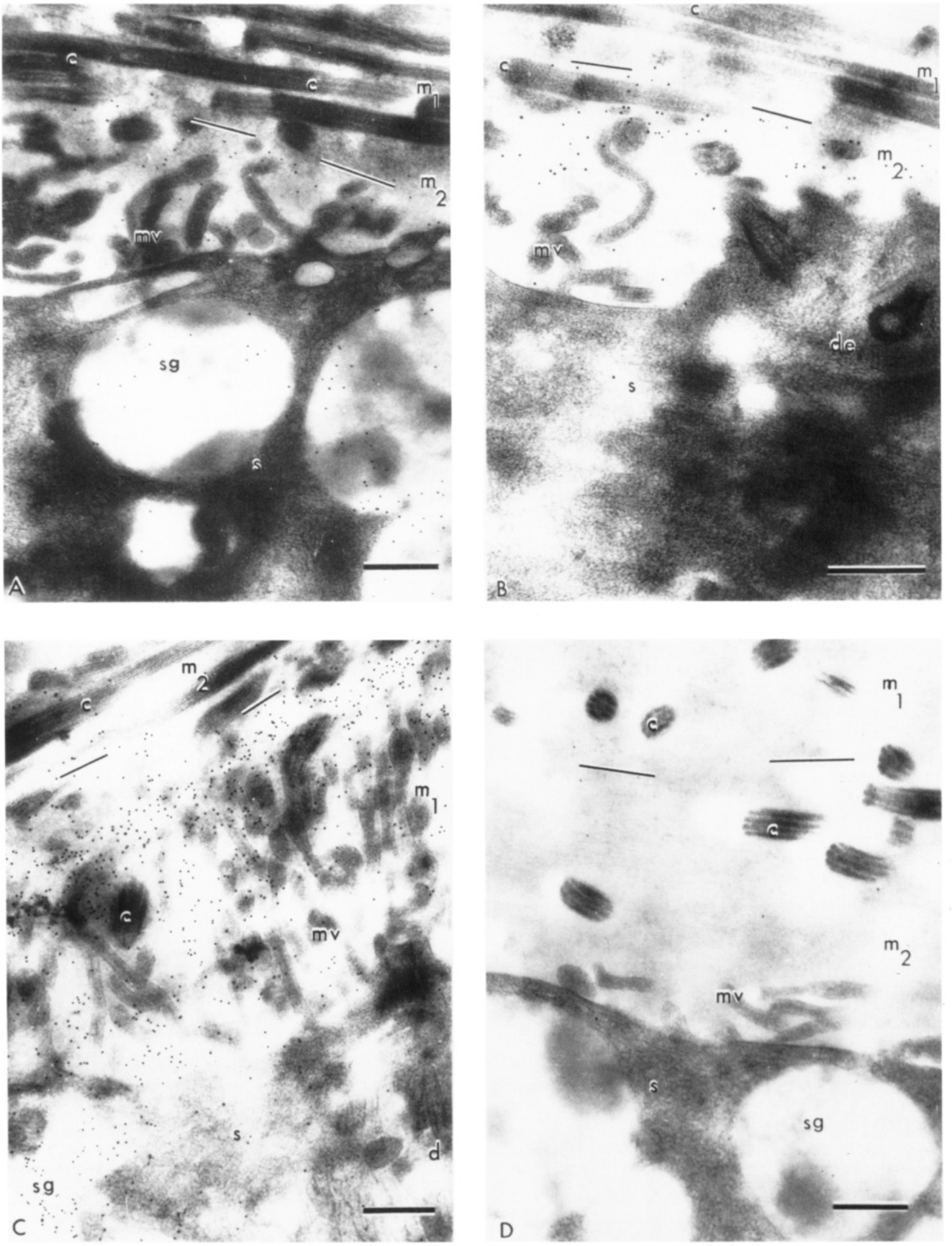

FIGURE 7: Electron micrographs of the surface of the olfactory neuroepithelium stained with anti-olfactomedin antibodies. Samples were incubated with polyclonal rabbit antibodies (panels A and B), mAb 43 (panel C), or preimmune serum (panel D). Olfactomedin is found in secretory granules of sustentacular cells and in the lower layer of the mucus, surrounding the microvilli of sustentacular cells, the dendritic knobs, and the proximal parts of olfactory cilia. The thin lines in the panels indicate the transition zone between the granular upper mucus layer (m_1) and the smooth lower mucus layer (m_2; Reese, 1965; Menco, 1980). sg, secretory granules; mv, microvilli; c, cilia; d, dendrite; de, dendritic ending; s, sustentacular cell. Bars represent 500 nm.

the dendritic cilia of olfactory receptor cells.

We extended our immunohistochemical studies to the electron microscopic level to obtain more detailed information about the deposition of olfactomedin at the epithelial surface. Electron micrographs of freeze-substituted samples reveal immunoreactivity in secretory granules of sustentacular cells and in the lower layer of the mucus, surrounding olfactory cilia, dendritic knobs, and microvilli of sustentacular cells, in line with light microscopic observations (Figure 7). Since the electron micrographs only visualize the epithelial surface, they do not provide information about localization of olfactomedin in the acinar cells of glands.

The function of olfactomedin remains to be determined. It is possible that olfactomedin represents a constituent of the mucous matrix, which lines the olfactory mucosa, and facilitates interactions between odorants and olfactory receptors at the ciliary membrane. Support for the notion that components of the mucus, like olfactomedin, may promote interactions between odorants and chemosensory cilia (Getchell et al., 1984) comes from the observation that responses from olfactory receptor cells can be elicited by picomolar concentrations of odorant in preparations that allow some mucus to remain associated with the olfactory cilia (Frings & Lindemann, 1990). Previous studies reported several proteins that bind radioactive odorants, such as anisole (Goldberg et al., 1979), androstenone (Gennings et al., 1977), camphor (Fesenko et al., 1978, 1979), and pyrazines (Pelosi et al., 1982; Bignetti et al., 1985; Pevsner et al., 1985). The pyrazine binding protein is the best characterized of these proteins and appears to be a member of a family of carrier proteins for hydrophobic ligands (Pevsner et al., 1988). A cDNA that encodes a homologue of this pyrazine binding protein expressed in Bowman's glands of frog olfactory tissue has also been identified (Lee et al., 1987). Olfactomedin appears to be distinct from these hydrophobic ligand carrier proteins, but bears resemblance to the previously described camphor binding protein (Fesenko et al., 1979). This protein was solubilized from bullfrog olfactory epithelium with Triton X-100 and had an apparent molecular weight of 120 kDa. It bound [^{3}H]-camphor with nanomolar affinity and binding of the odorant was greatly diminished by treatment with sulfhydryl reagents (Fesenko et al., 1978, 1979). Investigating the binding of odorants to olfactomedin and odorant-facilitated binding of olfactomedin to ciliary membranes along with molecular cloning of cDNA encoding olfactomedin and the elucidation of its primary structure eventually will clarify the role of this novel olfactory protein in vertebrate chemoreception.

Acknowledgments

We thank Kevan Mann and Sosena Kebede for their participation in this project and Dr. William D. Matthew for helpful suggestions and critical reading of the manuscript.

References

Anholt, R. R. H. (1989) *Am. J. Physiol. 257 (Cell Physiol. 26)*, C1043–C1054.

Anholt, R. R. H., & Rivers, A. M. (1990) *Biochemistry 29*, 4049–4054.

Anholt, R. R. H., Aebi, U., & Snyder, S. H. (1986) *J. Neurosci. 6*, 1962–1969.

Anholt, R. R. H., Mumby, S. M., Stoffers, D. A., Girard, P. R., Kuo, J. F., & Snyder, S. H. (1987) *Biochemistry 26*, 788–795.

Anholt, R. R. H., Petro, A. E., & Rivers, A. M. (1990) *Biochemistry 29*, 3366–3373.

Bakalyar, H. A., & Reed, R. R. (1990) *Science 250*, 1403–1406.

Bignetti, E., Cavaggioni, A., Pelosi, P., Persaud, K. C., Sorbi, R. T., & Tirindelli, R. (1985) *Eur. J. Biochem. 149*, 227–231.

Boekhoff, I., Tareilus, E., Strottman, J., & Breer, H. (1990) *EMBO J. 9*, 2453–2458.

Breer, H., Boekhoff, I., & Tareilus, E. (1990) *Nature 345*, 65–68.

Bridgman, P. C., & Daley, M. E. (1989) *J. Cell Biol. 108*, 95–109.

Buck, L., & Axel, R. (1991) *Cell 65*, 175–187.

Carlemalm, E., & Villiger, W. (1989) in *Techniques in Immunocytochemistry* (Bullock, G. R., & Petrusz, P., Eds.) Vol. 4, pp 29–45, Academic Press, London.

Dhallan, R. S., Yau, K. W., Schrader, K. A., & Reed, R. R. (1990) *Nature 347*, 184–187.

Duchamp, A., Revial, M. F., Holley, A., & MacLeod, P. (1974) *Chem. Senses Flavour 1*, 213–233.

Fesenko, E. E., Novoselov, V. I., Mjasedov, N. F., & Sidorov, G. V. (1978) *Stud. Biophys. 73*, 71–84.

Fesenko, E. E., Novoselov, V. I., & Krapivinskaya, L. D. (1979) *Biochim. Biophys. Acta 587*, 424–433.

Firestein, S., & Werblin, F. (1989) *Science 244*, 79–82.

Firestein, S., Darrow, B., & Shepherd, G. M. (1991) *Neuron 6*, 825–835.

Frings, S., & Lindemann, B. (1990) *Biophys. J. 57*, 1091–1094.

Frings, S., & Lindemann, B. (1991) *J. Gen. Physiol. 97*, 1–16.

Gennings, J. N., Gower, D. B., & Bannister, L. H. (1977) *Biochim. Biophys. Acta. 496*, 547–556.

Getchell, T. V., Margolis, F. L., & Getchell, M. L. (1984) *Prog. Neurobiol. 23*, 317–345.

Goldberg, S. J., Turpin, J., & Price, S. (1979) *Chem. Senses Flavour 4*, 207–214.

Goudswaard, J., Van der Donk, J. A., Noordzij, A., Van Dam, R. H., & Vaerman, J. P. (1978) *Scand. J. Immunol. 8*, 21–28.

Heuser, J. E., Reese, T. S., Dennis, M. J., Jan, Y., Jan, L., & Evans, L. (1979) *J. Cell Biol. 81*, 275–300.

Humbel, B., & Schwartz, H. (1989) *Immuno-Gold Labeling in Cell Biology* (Verkleij, A. J., & Leunissen, J. L. M., Eds.) pp 3–16, CRC Press, Boca Raton, FL.

Huque, T., & Bruch, R. C. (1986) *Biochem. Biophys. Res. Commun. 137*, 36–43.

Jones, D. T., & Reed, R. R. (1989) *Science 244*, 790–795.

Kolesnikov, S. S., Zhainazarov, A. B., & Kosopalov, A. V. (1990) *FEBS Lett. 266*, 96–98.

Kurahashi, T. (1990) *J. Physiol. 430*, 355–371.

Kurahashi, T., & Shibuya, T. (1990) *Brain Res. 515*, 261–268.

Laemmli, U. K. (1970) *Nature 227*, 680–685.

Lancet, D. (1986) *Annu. Rev. Neurosci. 9*, 329–355.

Lee, K. H., Wells, R. G., & Reed, R. R. (1987) *Science 235*, 1053–1056.

Lowry, O. H., Rosebrough, N. J., Farr, A. L., & Randall, R. J. (1951) *J. Biol. Chem. 193*, 265–275.

Menco, B. Ph. M. (1980) *Cell Tissue Res. 207*, 183–209.

Menco, P. Ph. M. (1989a) *Scanning Microsc. 3*, 257–272.

Menco, B. Ph. M. (1989b) *Cell Tissue Res. 256*, 275–281.

Nakamura, T., & Gold, G. H. (1987) *Nature 325*, 442–444.

Oakley, B. R., Kirsch, D. R., & Morris, N. R. (1980) *Anal. Biochem. 105*, 361–363.

Pace, U., & Lancet, D. (1986) *Proc. Natl. Acad. Sci. U.S.A. 83*, 4947–4951.

Pace, U., Hanski, E., Salomon, Y., & Lancet, D. (1985) *Nature 316*, 255–258.
Pelosi, P., Baldaccini, N. E., & Pisanelli, A. M. (1982) *Biochem. J. 201*, 245–248.
Pevsner, J., Trifiletti, R. R., Strittmatter, S. M., & Snyder, S. H. (1985) *Proc. Natl. Acad. Sci. U.S.A. 82*, 3050–3054.
Pevsner, J., Reed, R. R., Feinstein, P. G., & Snyder, S. H. (1988) *Science 241*, 336–339.
Pfeuffer, E., Mollner, S., Lancet, D., & Pfeuffer, T. (1989) *J. Biol. Chem. 264*, 18803–18807.
Phillips, T. E., & Boyne, A. F. (1984) *J. Electron Microsc. Tech. 1*, 9–29.
Reese, T. S. (1965) *J. Cell Biol. 25*, 209–230.
Restrepo, D., Miyamoto, T., Bryant, B. P., & Teeter, J. H. (1990) *Science 249*, 1166–1168.
Shirley, S. G., Robinson, C. J., Dickinson, K., Aujla, R., & Dodd, G. H. (1986) *Biochem. J. 240*, 605–607.
Sicard, G., & Holley, A. (1984) *Brain Res. 292*, 283–296.
Sitte, H., Neumann, K., & Edelmann, L. (1986) in *The Science of Biological Specimen Preparation for Microscopy and Microanalysis 1985* (Mueller, M., Becker, R. P., Boyde, A., & Wolose-wick, J. J., Eds.) pp. 103–108, Scanning Electron Microscopy, Inc., AMF O'Hare, Chicago, IL.
Sklar, B. P., Anholt, R. R. H., & Snyder, S. H. (1986) *J. Biol. Chem. 261*, 15538–15543.

Conformational Mobility of His-64 in the Thr-200 → Ser Mutant of Human Carbonic Anhydrase II[†,‡]

Joseph F. Krebs and Carol A. Fierke*
Department of Biochemistry, Duke University Medical Center, Box 3711, Durham, North Carolina 27710
Richard S. Alexander and David W. Christianson*
Department of Chemistry, University of Pennsylvania, Philadelphia, Pennsylvania 19104-6323
Received March 27, 1991; Revised Manuscript Received June 20, 1991

ABSTRACT: The three-dimensional structure of the Thr-200 → Ser (T200S) mutant of human carbonic anhydrase II (CAII) has been determined by X-ray crystallographic methods at 2.1-Å resolution. This particular mutant of CAII exhibits CO_2 hydrase activity that is comparable to that of the wild-type enzyme with a 2-fold stabilization of the $E{\cdot}HCO_3^-$ complex and esterase activity that is 4-fold greater than that of the wild-type enzyme. The structure of the mutant enzyme reveals no significant local changes accompanying the conservative T200S substitution, but an important nonlocal structural change is evident: the side chain of catalytic residue His-64 rotates away from the active site by 105° about χ_1 and apparently displaces a water molecule. The displaced water molecule is present in the wild-type enzyme; however, the electron density into which this water is built is interpretable as an alternate conformation of His-64 with 10–20% occupancy. The rate constants for proton transfer from the zinc–water ligand to His-64 and from His-64 to bulk solvent are maintained in the T200S variant; therefore, if His-64 is conformationally mobile about χ_1 and/or χ_2 during catalysis, compensatory changes in solvent configuration must sustain efficient proton transfer.

Human carbonic anhydrase II (CAII;[1] EC 4.2.1.1) is a zinc metalloenzyme containing one essential metal ion bound to a single polypeptide chain of 260 amino acids [for recent reviews, see Coleman (1986); Lindskog (1986); Silverman and Lindskog (1988), and Christianson (1991)]. The biological function of CAII in the erythrocyte is the hydration of carbon dioxide to form bicarbonate ion plus a proton. Since $k_{cat}/K_M = 1.5 \times 10^8$ M^{-1} s^{-1} for this enzyme, it appears to be one of only a few enzymes for which catalysis approaches the limit of diffusion control. However, since the biological mechanism of CAII requires a proton transfer from the enzyme to bulk solvent, the observed turnover rate of 10^6 s^{-1} requires the participation of buffer—ordinarily, proton transfer from an enzyme-bound group with $pK_a = 7$ to bulk solvent may proceed no faster than 10^3 s^{-1} (Eigen & Hammes, 1963).

The structure of native CAII from human blood has been determined by X-ray crystallographic methods (Liljas et al., 1972) and refined at 2.0-Å resolution (Eriksson et al., 1986, 1988a). The enzyme is roughly spherical and the active site lies at the bottom of a conical cleft about 15 Å deep. Important polar residues in the active site include Thr-199, Thr-200, Glu-106, and His-64; His-94, His-96, His-119, and hydroxide ion coordinate to Zn^{2+}. Additionally, a hydrophobic pocket is adjacent to the zinc–hydroxide species. Of the polar active-site residues, Glu-106 and Thr-199 engage zinc-bound hydroxide in a hydrogen-bond network (Eriksson et al., 1988a; Merz, 1990, 1991), Thr-200 interacts with CO_2 in a proposed

[†] D.W.C. thanks the NIH for Grant GM45614, the NSF for Grant DIR-8821184, the Chicago Community Trust for a Searle Scholar Award, and the Office of Naval Research for a Young Investigator Award. C.A.F. thanks the NIH for Grant GM40602, the American Cancer Society for Grant JFRA-246, and The David and Lucile Packard Foundation for a Fellowship in Science and Engineering.

[‡] The coordinates of T200S CAII, as well as those of the wild-type enzyme, have been deposited in the Brookhaven Protein Data Bank under reference codes 5CA2 and 4CA2, respectively.

[1] Abbrevations: IPTG, isopropyl β-D-thiogalactopyranoside; T200S, Thr-200 → Ser; T200H, Thr-200 → His; CAII, human carbonic anhydrase II; WT, wild type; PNPA, *p*-nitrophenyl acetate; MES, 2-(*N*-morpholino)ethanesulfonic acid; TAPS, [tris(hydroxymethyl)methyl]-3-aminopropanesulfonic acid; HEPES, *N*-(2-hydroxyethyl)piperazine-*N*'-2-ethanesulfonic acid; EDTA, (ethylenedinitrilo)tetraacetic acid; DNSA, dansylamide; ACET, acetazolamide.

0006-2960/91/0430-9153$02.50/0 © 1991 American Chemical Society